Materials and Methods

Plasmids

The cDNA encoding human Atg13 (KIAA0652/AB014552) was obtained from Kazusa DNA Research Institute in Japan. The cDNAs for human FIP200, mouse ULK1, and mouse ULK2 constructs were obtained from Open Biosystems (clones 3908134, 6834534, and 5709559 respectively). Human Atg101 and human ULK3 isoform 2 was obtained from Invitrogen (clones 60673 and IOH45122 respectively). The myc tag and attL1 sites (for BP reaction) were added by PCR to the N-terminus of ULK1 using the standard procedure. cDNAs were subcloned into pDONR221 with BP clonase (Invitrogen), and site-directed mutagenesis was performed using QuikChange II XL (Stratagene) according to the manufacturers instructions. Kinase dead ULK1 was achieved by a K46I mutation as previously described (*1*). Wild type and mutant alleles in pDONR221 were sequenced in their entirety to verify no additional mutations were introduced during PCR or mutagenesis steps and then put into either mammalian expression pDest15 GST bacterial expression vector, pcDNA3 myc mammalian expression vector, or pcDNA6.2 V5 dest (Invitrogen), or pQCXIN retroviral destination vector (Addgene 17399) by LR reaction (Invitrogen). pEBG-AMPK α1(1-312) is constitutively active by truncation after amino acid 312 and has been described previously (2). pEBG and pEBG-14-3-3 constructs (*3*) and human myc-Raptor constructs (described in ref. *4*) available from Addgene (plasmids#22227, 1942, 1859, 18118 respectively).

Antibodies and reagents

Cell Signaling Antibodies used: pAMPK Thr172 (#2535), AMPK α1 (#2532), AMPK α2 (2757) AMPK beta 1/2 (#4150), AMPK α1/2 (#2532), Atg5 (#2630), pACC Ser79 (#3661), ACC (3662), pRaptor Ser792 (#2083), pULK1 Ser467 (#4634), ubiquitin (#3933), Raptor (#2280), Myc poly (#2278), Myc 9B11 (#2276), COX IV (4844), GST (#2622), LC3B (#3868). Anti-ULK1 (A7481), M2 agarose (A2220) actin (A5441), and Flag poly (F7425) from Sigma. Guinea pig anti-p62 sequestosome antibody from Progen, Heidelberg Germany (03-GPP62-C). TOM20 antibody from Santa Cruz (FL-145). Phospho-ULK1 Ser555 was developed in collaboration with Gary Kasof at Cell Signaling Technology. GSH sepharose from GE Healthcare. Active recombinant AMPK was obtained from Millipore (cat#14-305). AICAR was obtained from Toronto Research Chemicals. Bafilomycin A, Phenformin, and metformin from Sigma and Phenformin and metformin were dissolved in DMEM with 10% FBS. Earle's Buffered Salk Solution (EBSS), Medium199 (for primary hepatocytes), Protein G sepharose, and Mitotracker Red CMXRos from Invitrogen. A769662 from Abbott Labs. Annexin V-PE Apoptosis Detection Kit from BD Biosciences, and JC-1 dye and CCCP from Molecular Probes. STO-609 from VWR. TPP plates for primary hepatocytes from Light Lab Systems.

shRNA target sequences:

TRC lentiviral shRNAs targeting ULK1 or ULK2 were obtained from Sigma.
Human ULK1 shRNA #5: TRCN0000000835
Human ULK1 shRNA #6: TRCN0000000836
Human ULK1 shRNA #7: TRCN0000000837
Human ULK1 shRNA #8: TRCN0000000838
Human ULK1 shRNA #9: TRCN0000000839
Human ULK2 shRNA #89: TRCN0000000889
Human ULK2 shRNA #90: TRCN0000000890

Human ULK2 shRNA #91: TRCN0000000891
Human ULK2 shRNA #92: TRCN0000000892
Human ULK2 shRNA #93: TRCN0000000893
Mouse ULK2 shRNA #20: TRCN0000278670
Mouse ULK2 shRNA #38: TRCN0000278671
Mouse ULK2 shRNA #65: TRCN0000026765
Mouse ULK2 shRNA #93: TRCN0000026693
Mouse ULK2 shRNA #95: TRCN0000026695

Cell Culture and Transfection

HEK293T, U2OS, and mouse embryonic fibroblast (MEF) cells were cultured in DMEM containing 10% fetal bovine serum (HyClone) and penicillin/streptomycin at 37°C in 5% CO_2. For transient expression of proteins and packaging of virus, HEK-293T cells were transfected with DNA or short hairpin RNA (shRNA) plasmids using Lipofectamine 2000 (Invitrogen) following the manufacturer's protocol. SV40 immortalized wild-type and ULK1 knockout MEFs were previously described (*5*). Primary ULK1 wt and -/- MEFs were isolated as previously described (*6*). Briefly, embryos were harvested, the heads and internal organs were removed, and the carcasses were finely minced with scissors and digested by incubation in 0.05% trypsin–0.5 mM EDTA solution for 30 min at 37°C with gentle agitation. Trypsin was inactivated by adding high- glucose Dulbecco modified Eagle medium (DMEM; Invitrogen, Carlsbad, CA) supplemented with 10% heat-inactivated fetal bovine serum (FBS; Invitrogen) and antibiotics. Homogeneous cell suspensions were plated in DMEM containing 10% FBS and maintained at 37°C as monolayer cultures. The genotype of each source of primary MEFs was determined by PCR. Primary wild-type and AMPKa1-/-, a2-/- double knockout MEFs were previously described (*6*).

Primary hepatocytes were isolated as previously described (*7*). Briefly, livers were perfused with Hank's balanced salt solution (HBSS, KCl, 5.4 mM;KH_2 PO_4 ,0.45mM; NaCl, 138mM; $NaHCO_3$,4.2 mM; Na_2HPO_4, 0.34 mM; glucose, 5.5 mM; HEPES, 1 M; EGTA, 50 mM; $CaCl_2$, 50 mM; pH 7.4). Livers were washed at a rate of 5 ml/min using the portal vein before collagenase (0.025%) was added. Cell viability was assessed by the trypan blue exclusion test and was always higher than 60%. Hepatocytes were seeded at a density of $2x10^6$ cells in medium M199 with Earle salts (Invitrogen), supplemented with 10 g/ml of streptomycin, 100 units/ml of penicillin, and 2.4 mM of glutamine onto TPP plates (Light Lab Systems). After cell attachment (6 h), the medium was replaced by fresh M199 medium for 24 h before indicated treatments.

For RNAi experiments, smartpools from Dharmacon against mouse ULK1, ULK2, or Atg5 (L-040155-00-0005, L-040619-00-0005, and L-064838-00-0005 respectively) were transfected at a final concentration of 20 nM according to the manufacturers instructions using RNAiMAX (Invitrogen). Cells were subsequently placed in EBSS or DMEM with 10% FBS media as a control for the indicated times, and were lysed 72 hours post-transfection. FACS analysis to analyze cell death described below.

Lenti- and retro-viral Preparation and Viral Infection

Lentiviral shRNA transduction and retroviral gene expression was performed as described previously (*4*). Briefly, for retroviral infection, the pQCXIN myc ULK1 constructs were transfected along with the ampho packaging plasmid into growing HEK293T cells. Virus-containing supernatants were collected 48 hours after transfection, filtered to eliminate cells and target ULK1 -/- MEFs or U2OS were infected in the presence of polybrene. 24 hours later, cells were selected with neomycin. The pLKO shRNA vectors encoding shRNAs

were transfected into HEK293T cells with lentiviral packaging plasmids vsvg, GAG/pol, and REV using Lipofectamine 2000. Viruses were collected 48 hours after transfection, and MEFs (shRNA #93 against mULK2) and U2OS (shRNA #8 and #91 against hULK1 and hULK2 respectively) already stably expressing myc-ULK1 were infected with the collected viruses for 4h in the presence of polybrene to knock down the endogenous proteins.

Cell lysis, immunoprecipitations, and mammalian autophagy analysis

Cells were harvested 24 hours after transfection for co-immunoprecipitation assay and Western blot analysis. Cells were rinsed once with ice-cold PBS and lysed in ice-cold lysis buffer (20mM Tris pH 7.5, 150mM NaCl, 1mM EDTA, 1 mM EGTA, 0.3% CHAPS, 2.5 mM pyrophosphate, 50 mM NaF, 5 mM b-glycero-phosphate, 50 nM calyculin A, 1 mM Na3VO4, and proteased inhibitors (Roche). The soluble fractions of cell lysates were isolated by centrifugation at 13,000 rpm for 10 minutes. For immunoprecipitations, primary antibodies were added to the lysates and incubated with rotation for 1.5 hours at 4°C. 60 µl of a 50% slurry of protein G-sepharose was then added and the incubation continued for an additional 1 hour. Immunoprecipitates were washed three times with cold lysis buffer before addition of sample buffer. Immunoprecipitated proteins were denatured by the addition of 20 µl of sample buffer and boiling for 5 minutes, resolved by 8%–16% SDS-PAGE, and analyzed by immunoblotting as described. For analysis of autophagy by western blots, cells were plated at a density of $2.0x10^5$ per dish in 6cm dishes and grown in DMEM plus 10% FBS, penicillin, and streptomycin. Twenty hours after plating, the growth medium was replaced with aforementioned medium (ctl), or starvation (EBSS) for the indicated times with or without 100 nM bafilomycin A and lysed in boiling lysis buffer (10mM Tris pH7.5, 100mM NaCl, 1% SDS). After trituration, lysates were equilibrated for protein levels using the BCA method (Pierce) and resolved on 6 to 12% SDS-PAGE gels, depending on the experiment. Quantification of westerns blots was achieved using Kodak Multi Gage software and normalizing to the appropriate loading control (actin when comparing p62 or LC3, or total protein level when comparing phospho-specific antibodies). In all cases, starvation is EBSS (Earle's Buffered Salt Solution) (Invitrogen). Data shown from all cell experiments is representative of 3 independent experiments.

AMPK and ULK1 Kinase Assays

Gamma 32P assays to measure ULK1 kinase activity were performed as previously described (8). Briefly, myc ULK1 was transfected into HEK293T cells and 20 hours later treated as indicated. The immmunoprecipitate was washed in IP buffer 3 times, and washed in kinase buffer (25 mM MOPS, pH 7.5, 1 mM EGTA, 0.1 mM Na_3VO_4, 15 mM $MgCl_2$,). ATP was added at a 100 µM final concentration. Reactions were performed for 20 minutes at 30°C. Reactions were boiled, run out on SDS page gel. The gel was dried, and imaged using PhosphoImager software. In vitro kinase assays to asses AMPK activity on ULK1 were performed using the same protocol as above, but using 0.1 U per rxn of partially purified rat liver active AMPK heterotrimer (Millipore cat#14-305) and ~1ug of purified myc-tagged ULK1 or ~ 2ug of myc-tagged Raptor in a reaction containing 50 mM Tris pH 7.5 and 10 mM $MgCl_2$ at 30°C for 15 minutes. The units here are 1380U/mg where one unit of AMPK activity is defined as 1 nmol of phosphate incorporated into 200uM of the AMARA substrate peptide (AMARAASAAALARRR) per minute at 30 degrees C with a final ATP concentration of 100uM. Myc-tagged Raptor or ULK1 was purified from transiently transfected plates of HEK293T cells. The amount of immunoprecipitated Raptor or ULK1 was initially estimated from comparing the colloidal blue stained amount of immunoprecipitated protein per 10cm plate lysed and compared to BSA standards.

Quantification of ^{32}P signal was done using PhosphoImager and Kodak Multi Gage software. For cold assays AMPK assays, reactions were run out on SDS page gel, transferred, and blotted with a phospho-specific antibody against either serine467 or 555 of ULK1.

Fluorescence Microscopy Methods

MEFs reconstituted with myc ULK1 were plated on glass coverslips at a density of $3x10^5$ cells per well in 6-well tissue culture plates. 18h later, cells were fixed in 4% PFA in PBS for 10 minutes and permeabilized in 0.2% Triton in PBS for 10 minutes. The following primary antibodies were used: mouse anti-myc epitope and LC3B XP antibody (2276 and 3868 respectively, Cell Signaling Technologies). Secondary antibodies were anti-rabbit Alexa488 and anti-mouse Alexa594 (Molecular Probes, 1:1000). Mitotracker Red CMXRos (Invitrogen) was added to live cells at a concentration of 50 nM for 15 minutes. Coverslips were mounted in FluoromountG (SouthernBiotech). 10 random fields per condition were acquired using the 100x objective and representative images shown. Primary hepatocytes were isolated from ULK1 -/-, AMPKa1-/-, a2-/- double knockout, or matched wt littermates and the cells were plated at confluency on TPP plates, then 48 hours washed with PBS and fixed in 4% cold PFA 20 hours later. TOM20 (FL-145) used according to the manufacturers instructions at 1:200 overnight incubation at 4 degrees. Glass coverslips were mounted directly on plate with FluoromountG.

All confocal microscopy was performed on an LSM 710 spectral confocal microscope mounted on an inverted Axio Observer Z1 frame (Carl Zeiss, Jena, Germany). LC3 puncta were labeled with anti LC3B (#3868 from Cell Signaling Technology) and counterstained with DAPI. Excitation for both markers was provided by a 405nm solid-state diode laser (for DAPI) and the 488nm line of an Argon-ion laser (for green) respectively. Laser light was directed to the sample via two separate dichroic beamsplitters (HFT 405 and HFT 488) through a Plan-Apochromat 63X 1.4NA oil immersion objective (Carl Zeiss, Jena Germany). Fluorescence was epi-collected and directed to the detectors via a secondary dichroic mirror. DAPI fluorescence was detected via a photomultiplier tube (PMT) using the spectral window 430-480nm. Green fluorescence was detected on a second photomultipler tube (PMT) with a detection window of 500-570nm. Confocal slice thickness was typically kept at 0.8 microns consistently for both fluorescence channels with 10 slices typically being taken to encompass the three-dimensional entirety of the cells in the field of view. Maximum intensity projections of each region were calculated for subsequent quantification and analysis.

Quantifying Endogenous LC3 puncta

In order to quantify the endogenous LC3 puncta, which were stained with anti LC3 antibody (Cell Signaling #3868), an ImageJ macro was utilized (refs. 9 and 10). Briefly, an individual cell within a field of view was selected via the polygon tool. The RGB image is split into its component red, green and blue channels, with the green channel being extracted to an 8-bit grayscale format. This image was then thresholded to two standard deviations above the background signal. Care was taken to ensure consistency of thresholding over multiple fields of view and samples. Once thresholded, the grayscale image was photographically inverted to black pixels over a white background. Once this process was complete, the analyze particles algorithm within ImageJ was employed to measure the number of puncta within a specified region of interest (ie a single cell). This process was completed for at least 6 cells within over 10 separate fields of view for each sample and is representative of 3 independent experiments.

Electron Microscopy

Primary hepatocytes grown on TPP plates or MEFs grown in 60mm plastic culture dishes were fixed in 2.5% glutaraldehyde in 0.1M Na cacodylate buffer (pH7.3), washed and fixed in 1% osmium tetroxide in 0.1M Na cacodylate buffer. They were subsequently treated with 0.5% tannic acid followed by 1% sodium sulfate in cacodylate buffer and then dehydrated in graded ethanol series. The cells were transitioned in HPMA (2-hydroxypropyl methacrylate: Ladd Research, Williston VT) and embedded in LX112 resin. Following overnight polymerization at 60 degrees C, small pieces of resin were attached to blank blocks using SuperGlue. Thin sections (70nm) were cut on a Reichert Ultracut E (Leica, Deerfield, IL) using a diamond knife (Diatome, Electron Microscopy Sciences, Hatfield PA), mounted on parlodion coated, copper, slot grids and stained in uranyl acetate and lead citrate. Sections were examined on a Philips CM100 TEM (FEI, Hillsbrough, OR) and data documented on Kodak SO-163 film for later analysis. Alternatively the samples were documented on an Olympus- SIS Megaview III CCD camera (Lakewood, CO). For quantification of mitochondria, TEM micrographs were imported into CRI (Cambridge Research & Instrumentation) image analysis software inForm (version 1.0.0). The intracellular compartments for the nucleus and cytoplasm and the mitochondria were pseudocolored and segmented for quantification. Non-cell-containing image areas were subtracted from the analysis. Calculation for the adjusted total mitochondrial area per cell was as follows: (percent area mitochondria)/((percent area cytoplasm + percent area mitochondria)-(percent area nucleus)). Error bars shown are equal to mean +/- Standard Error of the Mean (SEM) N=10.

Mass Spectrometry

Myc-ULK1 overexpressed in HEK293T cells was treated with vehicle or 5 mM phenformin for 1 hour, IP'd with anti myc antibody (Cell Signaling), run out on SDS-PAGE gel and coomassie stained. Bands on the gel corresponding to ULK1 were cut out and subjected to reduction with dithiothreitol, alkylation with iodoacetamide, and in-gel digestion with trypsin or chymotrypsin overnight at pH 8.3, followed by reversed-phase microcapillary/tandem mass spectrometry (LC/MS/MS). LC/MS/MS was performed using an Easy-nLC nanoflow HPLC (Proxeon Biosciences) with a self-packed 75 μm id x 15 cm C_{18} column coupled to a LTQ-Orbitrap XL mass spectrometer (Thermo Scientific) in the data-dependent acquisition and positive ion mode at 300 nL/min. Peptide ions from AMPK predicted phosphorylation sites were also targeted in MS/MS mode for quantitative analyses. MS/MS spectra collected via collision induced dissociation in the ion trap were searched against the concatenated target and decoy (reversed) single entry ULK1 and full Swiss-Prot protein databases using Sequest (Proteomics Browser Software, Thermo Scientific) with differential modifications for Ser/Thr/Tyr phosphorylation (+79.97) and the sample processing artifacts Met oxidation (+15.99), deamidation of Asn and Gln (+0.984) and Cys alkylation (+57.02). Phosphorylated and unphosphorylated peptide sequences were identified if they initially passed the following Sequest scoring thresholds against the target database: 1+ ions, Xcorr ≥ 2.0 Sf ≥ 0.4, P ≥ 5; 2+ ions, Xcorr ≥ 2.0, Sf ≥ 0.4, P ≥ 5; 3+ ions, Xcorr ≥ 2.60, Sf ≥ 0.4, P ≥ 5 against the target protein database. Passing MS/MS spectra were manually inspected to be sure that all **b-** and **y-** fragment ions aligned with the assigned sequence and modification sites. Determination of the exact sites of phosphorylation was aided using FuzzyIons and GraphMod and phosphorylation site maps were created using ProteinReport software (Proteomics Browser Software suite, Thermo

Scientific). False discovery rates (FDR) of peptide hits (phosphorylated and unphosphorylated) were estimated below 1.5% based on reversed database hits.

Relative Quantification of Phosphorylation Sites

For relative quantification of phosphorylated peptide signal levels, an isotope-free (label-free) method was used by first integrating the total ion counts (TIC) for each MS/MS sequencing event during a targeted ion MS/MS (TIMM) experiment or a data-dependant acquisition. For each targeted phosphorylation site, a ratio of phosphorylated peptide signal (TIC of phosphorylated form) to the total peptide signal (TIC of phosphorylated form + TIC of non-phosphorylated form) for both the insulin and insulin plus rapamycin treated samples were calculated according to the following equation:

$$TIC_{PO4}/(TIC_{PO4}+TIC_{nonPO4}) = \text{Ratio of phosphopeptide signal } (R_{PO4})$$

These ratios of phosphopeptide signal were then compared to the same phosphopeptide ratios from the unstimulated samples according to the following equation:

$$[(R_{PO4}\text{Unstimulated}/R_{PO4}\text{Stimulated})-1] \times 100 = \%\ \text{change in phosphorylation level upon treatment}$$

While a direct comparison of phosphopeptide signals between different experimental conditions is not accurate due to differences in sample content, a comparison of the relative ratios of the phosphorylated to non-phosphorylated peptide forms between samples is an accurate measure of signal-level change since the total peptide signal (modified and unmodified) is measured. The above calculations were performed manually using Microsoft Excel and with automated in-house developed software named Protein Modification Quantifier v1.0 (Beth Israel Deaconess Medical Center, Boston, MA) (*11*).

Mice Strains and Tissue Isolation

AMPKa1$^{-/-}$ mice (*12*) and AMPKa2 $^{lox/lox}$ (*13*) were serially crossed onto the FVB strain for 4 generations and then intercrossed to generate AMPKa1$^{+/-}$ AMPKa2 $^{lox/+}$ and AMPKa1$^{-/-}$ AMPKa2 $^{lox/lox}$ littermates. 8 week old male mice were tail-vein injected with adenovirus bearing Cre-recombinase as previously described (*14*). Deletion of AMPKa2 was examined by immunoblotting with AMPKalpha antibodies which recognize both AMPKalpha1 and AMPKalpha2. ULK1-/- mice (*5*) were also crossed onto the FVB background for 3 generations prior to analysis. Experimental mice were cervically dislocated and liver and muscle were harvested immediately and either processed for histological analysis (10% formalin) or frozen in liquid nitrogen for molecular studies. These samples were then placed frozen into Nunc tubes, pulverized in liquid nitrogen, and homogenized in lysis buffer (20mM Tris pH 7.5, 150mM NaCl, 1mM EDTA, 1 mM EGTA, 1% Triton X-100, 2.5 mM pyrophosphate, 50 mM NaF, 5 mM -glycero-phosphate, 50 nM calyculin A, 1 mM Na3VO4, 10 mM PMSF, 4 µg/ml leupeptin, 4 µg/ml pepstatin, 4 µg/ml aprotinin) on ice for 30s using a tissue homogenizer. Total protein was normalized using BCA protein kit (Pierce) and lysates resolved on SDS-PAGE gel.

Flow Cytometry

Cells were seeded at a concentration of 2.5 x 10^5 cells/mL, grown overnight (18hrs) and treated with Vehicle (DMEM + 10%FBS) or EBSS or CCCP (100uM). Cells were collected at the appropriate time point, washed once in PBS, trypsinized and spun. For the JC-1 staining cells were resuspended in 1mL DMEM + 10% FBS, and stained with 2µM JC-1 dye

(Molecular Probes) at 37°C for 20 minutes in the dark. Cells were washed once and resuspended in 500μL staining buffer (PBS + 3% FBS). For Annexin V staining, cells were washed in 1x Annexin V buffer and treated as described by the Annexin V staining protocol (BD Pharmingen, San Diego, CA). Briefly, cells were resuspended in Annexin V buffer to a concentration of one million per mL, 100,000 cells were then stained with 5 μL of phycoerythrin (PE)-conjugated Annexin V antibody (BD Pharmingen) and 5 μL of 7-amino-actinomycin D (7AAD) and then incubated at room temperature for 15 minutes. 400μL of Annexin V buffer was then added to each sample with gentle mixing. Stained cells were analyzed using a FACScan flow cytometer (Becton Dickinson, San Jose, CA). Flow cytometry data was analyzed using FlowJo 8.6 software (Tree Star Inc., Ashland, OR).

Histology and Immunohistochemistry

Mouse tissues were fixed in 10% formalin overnight and embedded in paraffin. For immunohistochemistry, slides were deparaffinized in xylene and ethanol and rehydrated in water. Heat mediated antigen retrieval using sodium citrate pH 6.0 buffer and slides were quenched in hydrogen peroxide (3%) to block endogenous peroxidase activity and washed in TBST buffer. Slides were blocked in 5% normal serum for 1 hr at room temperature and incubated with primary antibody diluted in blocking buffer, washed and a secondary biotinylated goat-anti mouse IgG antibody was applied. The avidin-biotin peroxidase complex method (Vector, Burlingame, CA) was used and staining was visualized using the DAB chromophore (Vector ABC; DAB). Slides were counterstained with hematoxylin and mounted with Fluoromount (SoutherBiotech, Birmingham, AL). The anti-ubiquitin (P4D1) (Cell Signaling Technology, Beverly, MA 1:750) and anti-p62 (Progen, Heidelberg Germany 1:200) antibodies were diluted according to manufacturer's suggestions and as previously described (*23*). Images of p62 and ubiquitin shown in Fig. S7 representative of 2 independent experiments with 5 mice of each genotype analyzed.

Analysis of autophagic events in *C. elegans*

The level of autophagy in various mutant strains was assessed using a GFP::LGG-1/LC3 translational reporter, which was originally constructed and described in (15) and later integrated (DA2123 (*adIs2122[lgg1p::GFP:LGG1 + rol6])* (16). New strains used in this study were MAH14 (*daf-2(e1370) III; adIs2122[lgg1p::GFP:LGG1 + rol6]),* MAH28 *(aak2(ok524) X; adIs2122[lgg1p::GFP::LGG1 + rol6] and* AGD383 (*uthIs202[aak2cp::AAK2(aa1321)::TOMATO + rol6*]). AGD383 crossed to DA2123 to obtain F1 heterozygous animals used for scoring. AAK-2 gain of function expression construct consisted of the 3KB putative promoter region 5' to the *aak2*c (T01C8.1c) start site driving cDNA sequence corresponding to AAK-2 aa 1-321. Expression construct backbone was based upon pPD95.77 from the Fire lab *C. elegans* vector kit with tdTOMATO in place of GFP. Transgenic strains were generated via microinjection of 150 ug/ul DNA into the gonad of adult hermaphrodites using standard techniques with pRF4 *rol6(su1006)* a transformation marker. Integrated transgenic lines were generated using gamma irradiation and outcrossed to wild type (N2) animals four times. GFP-positive foci/puncta were counted as described earlier (*17*). In brief, GFP-positive foci were counted (using 1000-fold magnification on a Zeiss Axioplan II microscope) in the hypodermal seam cells of L3 transgenic animals, which were staged by gonad morphology and germline developmental phenotype. Between 3-10 seam cells were examined in each of 8-30 animals from at least two independent trials and averaged. Data analysis was done using unpaired, two-tailed *t*-test. When performing RNAi experiments to count GFP positive foci,

young adults were fed the RNAi bacteria, and the L3 progeny of their progeny ("F2 generation") were examined. When scoring heterozygote animals, AGD383 was raised on RNAi before being crossed, and L3 heterozygotes were subsequently analyzed. In all cases, animals were raised at 20ºC. RNAi clones were from Julie Ahringer's RNAi library (*18*) or Marc Vidal's RNAi library (*19*).

Statistical Analysis

Comparisons were made using the unpaired Student's *t*-test. SEM +/- is represented as error bars. Statistical significance as indicated.

Supplement References

1. Chan, EY, Longatti, A, McKnight, NC, and Tooze, SA. Kinase-inactivated ULK proteins inhibit autophagy via their conserved C-terminal domains using an Atg13-independent mechanism. Mol Cell Biol *29*, 157-171 (2009).

2. Crute BE, Seefeld K, Gamble J, Kemp BE, Witters LA. Functional Domains of the a1 Catalytic Subunit of the AMP-activated Protein Kinase. JBC 273(52), 35347-35354 (1998).

3. Tzivion G, Luo Z, and Avruch J. A dimeric 14-3-3 protein is an essential cofactor for Raf kinase activity. Nature 394 (6688), 88-92 (1998).

4. Gwinn DM, Shackelford DB, Egan DF, Mihaylova MM, Mery A, Vasquez DS, Turk BE, Shaw RJ. AMPK phosphorylation of raptor mediates a metabolic checkpoint. *Mol Cell* 30 (2), 214 (2008).

5. Kundu M, Lindsten T, Yang CY, Wu J, Zhao F, Zhang J, Selak MA, Ney PA, Thompson CB. Ulk1 plays a critical role in the autophagic clearance of mitochondria and ribosomes during reticulocyte maturation. Blood. 2008 Aug 15;112(4):1493-502.

6. Laderoute KR, Amin K, Calaoagan JM, Knapp M, Le T, Orduna J, Foretz M, and Viollet B. (2006). 5'-AMP-Activated Protein Kinase (AMPK) Is Induced by Low-Oxygen and Glucose Deprivation Conditions Found in Solid-Tumor Microenvironments. Mol Cell Biol 26, 5336-5347.

7. Dentin R, Pégorier JP, Benhamed F, Foufelle F, Ferré P, Fauveau V, Magnuson MA, Girard J, Postic C. Hepatic glucokinase is required for the synergistic action of ChREBP and SREBP-1c on glycolytic and lipogenic gene expression. J Biol Chem 279 (19), 20314-26 (2004).

8. Jung CH, Jun CB, Ro SH, Kim YM, Otto NM, Cao J, Kundu M, Kim DH. ULK-Atg13-FIP200 complexes mediate mTOR signaling to the autophagy machinery. Mol Biol Cell. 2009 Apr;20(7):1992-2003.

9. Chu CT, Plowey ED, Dagda RK, Hickey RW, Cherra III SJ, and Clark RS. Autophagy in Neurite Injury and Neurodegeneration: in vitro and in vivo models. Meth. Enzymol, 453:217-49, (2009)

10. Dagda RK, Zhu J, Kulich SM, and Chu CT. Mitochondrially localized ERK2 regulates mitophagy and autophagic cell stress. Autophagy. 4 (6), 770-82, 2008.

11. Yang X, Friedman A, Nagpal S, Perrimon N, Asara JM. Use of a label-free quantitative platform based on MS/MS average TIC to calculate dynamics of protein complexes in insulin signaling. J Biomol Tech. 2009 Dec;20(5):272-7.

12. Jørgensen SB, Viollet B, Andreelli F, Frøsig C, Birk JB, Schjerling P, Vaulont S, Richter EA, Wojtaszewski JF. Knockout of the alpha2 but not alpha1 5'-AMP-activated protein kinase isoform abolishes 5-aminoimidazole-4-carboxamide-1-beta-4-ribofuranoside but not contraction-induced glucose uptake in skeletal muscle. J Biol Chem 279 (2) 1079-9.

13. Andreelli F, Foretz M, Knauf C, Cani PD, Perrin C, Iglesias MA, Pillot B, Bado A, Tronche F, Mithieux G, Vaulont S, Burcelin R, Viollet B. Liver adenosine monophosphate-activated kinase-alpha2 catalytic subunit is a key target for the control of hepatic glucose production by adiponectin and leptin but not insulin. Endocrinology 147(5), 2432–2441 (2006).

14. Shaw RJ, Lamia KA, Vasquez D, Koo SH, Bardeesy N, Depinho RA, Montminy M, Cantley LC. The kinase LKB1 mediates glucose homeostasis in liver and therapeutic effects of metformin. Science. 310(5754):1642-6 (2005).

15. Meléndez A, Tallóczy Z, Seaman M, Eskelinen EL, Hall DH, Levine B. Autophagy genes are essential for dauer development and life-span extension in C. elegans. Science. 2003 Sep 5;301(5638):1387-91.

16. Kang C, You YJ, Avery L. Dual roles of autophagy in the survival of Caenorhabditis elegans during starvation. Genes Dev. 2007 Sep 1;21(17):2161-71.

17. Hansen M, Chandra A, Mitic LL, Onken B, Driscoll M, Kenyon C. A role for autophagy in the extension of lifespan by dietary restriction in C. elegans. PLoS Genet 4(2):e24 (2008).

18. Kamath RS, Fraser AG, Dong Y, Poulin G, Durbin R, Gotta M, Kanapin A, Le Bot N, Moreno S, Sohrmann M, Welchman DP, Zipperlen P, Ahringer J. Systematic functional analysis of the Caenorhabditis elegans genome using RNAi. Nature. 2003 Jan 16;421(6920):231-7.

19. Rual JF, Ceron J, Koreth J, Hao T, Nicot AS, Hirozane-Kishikawa T, Vandenhaute J, Orkin SH, Hill DE, van den Heuvel S, Vidal M. Toward improving Caenorhabditis elegans phenome mapping with an ORFeome-based RNAi library. Genome Res. 2004 Oct;14(10B):2162-8.

20. Asara JM, Christofk HR, Freimark LM, Cantley LC. A label-free quantification method by MS/MS TIC compared to SILAC and spectral counting in a proteomics screen. Proteomics (2008) vol. 8 (5) pp. 994-9

21. Dorsey FC, Rose KL, Coenen S, Prater SM, Cavett V, Cleveland JL, Caldwell-Busby J. Mapping the phosphorylation sites of Ulk1. J Proteome Res 2009; 8(11), 5253-63.

22. Williams T, Forsberg L, Viollet B, and Brenman J. Basal autophagy induction without AMP-activated protein kinase under low glucose conditions. Autophagy (2009) vol. 5 (8).

23. Waguri, S, and Kosmatsu, M. Biochemical and morphological detection of inclusion bodies in autophagy-deficient mice. Methods Enzymol 2009; 453, 181-196.

Figure S1

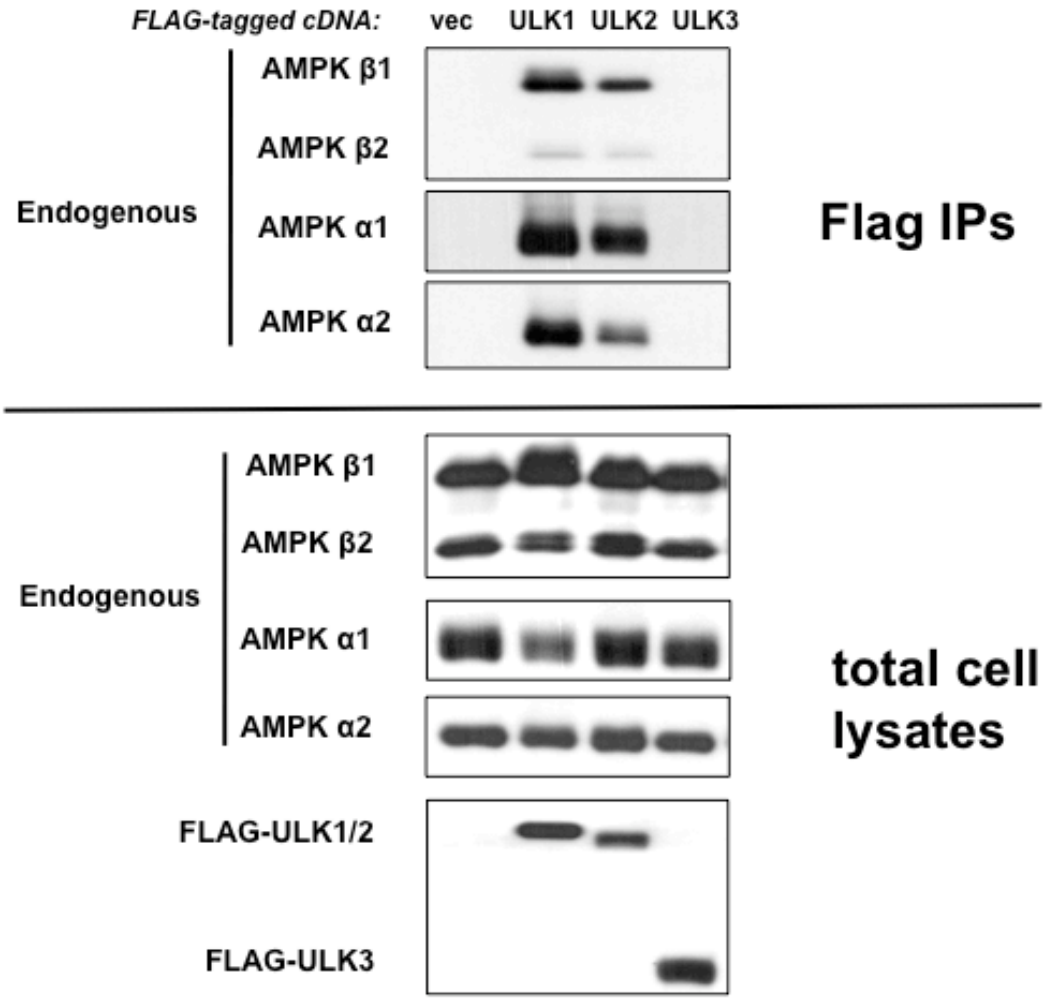

Fig. S1. ULK1 and ULK2, but not ULK3 co-immunoprecipitate with endogenous AMPK. Immunoprecipitates of FLAG-tagged ULK1, ULK2, ULK3 or empty FLAG-tagged vector (vec) transfected in HEK-293T cells were immunoblotted for endogenous AMPK subunits as indicated. Data is representative of 3 independent experiments.

Figure S2

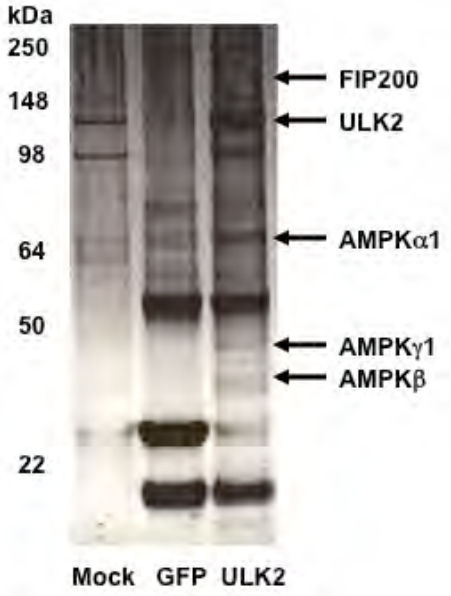

Protein ID by MS	Mascot score	# peptides
ULK2	3873	29 peptides
FIP200	138	5 peptides
AMPKα1	182	2 peptides
AMPKβ1	118	3 peptides
AMPKβ2	53	1 peptide
AMPKγ1	288	4 peptides

Fig. S2. Identification of endogenous AMPK as an interacting partner of ULK2
Eluted FLAG-tagged ULK2 immunoprecipitates from HEK-293T cells were resolved on SDS-PAGE and lanes 1 (mock transfected) and 3 (ULK2) of SuproRuby stained gel shown were sliced into 25 fragments each and analyzed by tandem mass spectrometry. Endogenous FIP200 as well as the indicated AMPK subunits were uniquely found in the ULK2 immunoprecipitates and bands corresponding to each in the ULK2 lanes are indicated. Mascot scores are indicated as well as number of unique peptides analyzed.

Figure S3

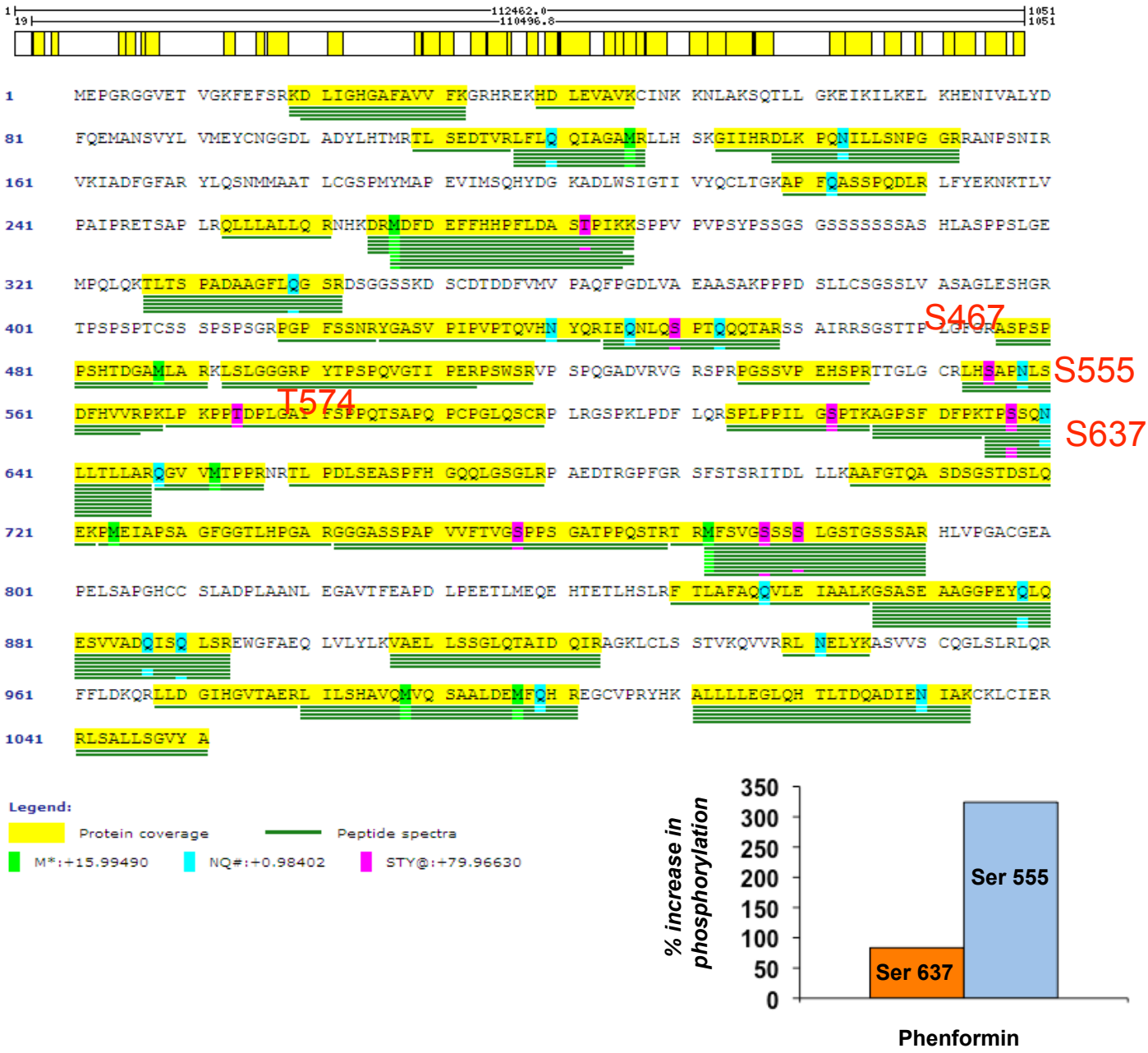

Fig. S3. Diagram of all LC/MS/MS identified in vivo phosphorylation sites in human ULK1. Top: Myc-ULK1 was transfected into human embryonic kidney (HEK)-293T cells, treated with 5 mM phenformin to reduce cellular ATP for 1 hour and immunoprecipitated with anti myc antibody. The IP was run out on SDS PAGE, stained with coomassie, and the band corresponding to myc-ULK1 was cut out, and isolated and subjected to tryptic digest and LC/MS/MS analysis. Three indicated sites matching the AMPK substrate motif were identified, all mapping to the serine – rich unstructured region between the N-terminal kinase domain and the conserved C-terminus that mediates ULK1 binding to its subunits Atg13 and FIP200. Bottom: Quantitative mass spec spectrometry (MS/MS TIC ratio quantification (ref. 20)) reveals that tryptic peptides containing Phospho- Ser_{555} and Phospho-Ser_{637} of ULK1 are induced by treatment of HEK-293T cells with 5mM phenformin for 1h.

Figure S4

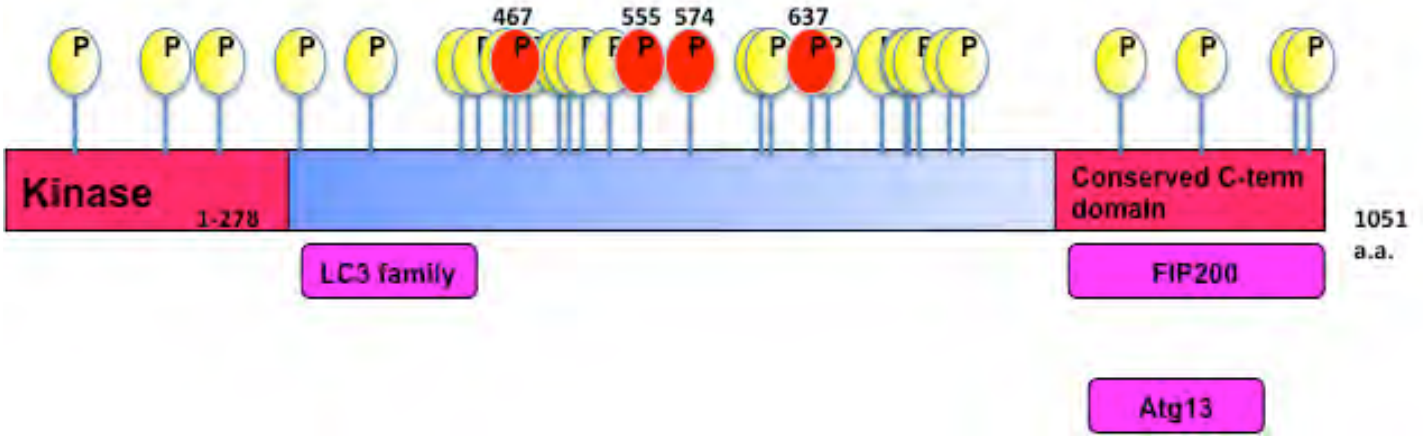

In vivo phosphorylation sites by mass spec

Ser 87	QEMANsVYLV
Ser 195	PEVIMsQHY
Ser 224	APFQAsSPQDL
Thr 281	PFLDAsTPIKK
Ser 341	GFLQGsRDSG
Ser 450*	EQNLQsPTQQQ
Thr 456	PTQQQtARSSA
Ser 465	SAIRRsGSTTP
Ser 467	IRRSGsTTPLG
Thr 469	RSGSTtPLGFG
Ser 477	GFGRAsPSPPS
Ser 479	GRASPsPPSHT
Ser 521	WSGTPsPQGAE
Ser 555*	GCRLHsAPNLS
Thr 574	LPKPPtDPLGA
Ser 622*	PPILGsPTKAG
Thr 624	ILGSPtKAGPS
Ser 637*	FPKTPsSQNLL
Ser 638	PKTPSsQNLLT
Thr 717	PDPGStESLQ
Ser 747	GGGASsPAPVV
Ser 757*	VFTVGsPPSGA
Ser 760	VGSPPsGATPF
Thr 763	PPSGAtPPQST
Ser 777	MFSVGsSSSLG
Ser 780	VGSSSsLGSTG
Ser 867	LKGSAsEAAG
Ser 913	VAELLsSGLQ
Ser 1043	IERRLsALLT
Thr 1047	LSALLtGICA
	Our data +phen
	Published
	*also published

Candidate AMPK sites:

> Ser 467: IRRSG**S**TTPL

> Ser 555: GCRLH**S**APNL

> Thr 574: LPKPP**T**DPLG

> Ser 637: FPKTP**S**SQNL

Fig. S4. Schematic of potential AMPK-dependent phosphorylation sites in ULK1. Results from Supplemental figure 3 shown along with previously published data. Previously published sites (www.Phosphosite.org, and ref. 21) indicated in green and sites identified in this work as being enriched in phenformin treated samples in yellow.

Figure S5

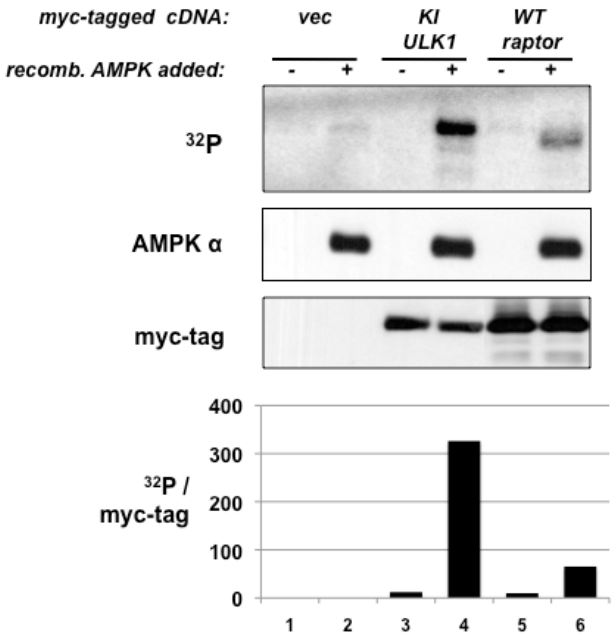

Fig. S5. Myc-tagged ULK1 is phosphorylated by exogenous AMPK in vitro.
In vitro kinase assays (from Fig. 1C) using purified Myc-tagged kinase-inactive (KI: K46I) ULK1 or myc- tagged wild-type raptor as substrates. Myc-tagged proteins (1-2ug per rxn) were produced in HEK-293T cells, purified, and subjected to an in vitro kinase assay in the presence of radioactive ^{32}P-γ-ATP with or without recombinant active heterotrimeric AMPK added as indicated (0.1 U per rxn). The kinase assays were resolved and parallel non-radioactive kinase assays were immunoblotted with AMPK alpha or myc-tag antibodies as indicated. ^{32}P signal was captured on a phosphoimager and its signal, as well as that of the anti-myc immunoblot, was densitometrically quantified and expressed as a ratio of ^{32}P incorporated per mol myc-tagged protein.

Figure S6

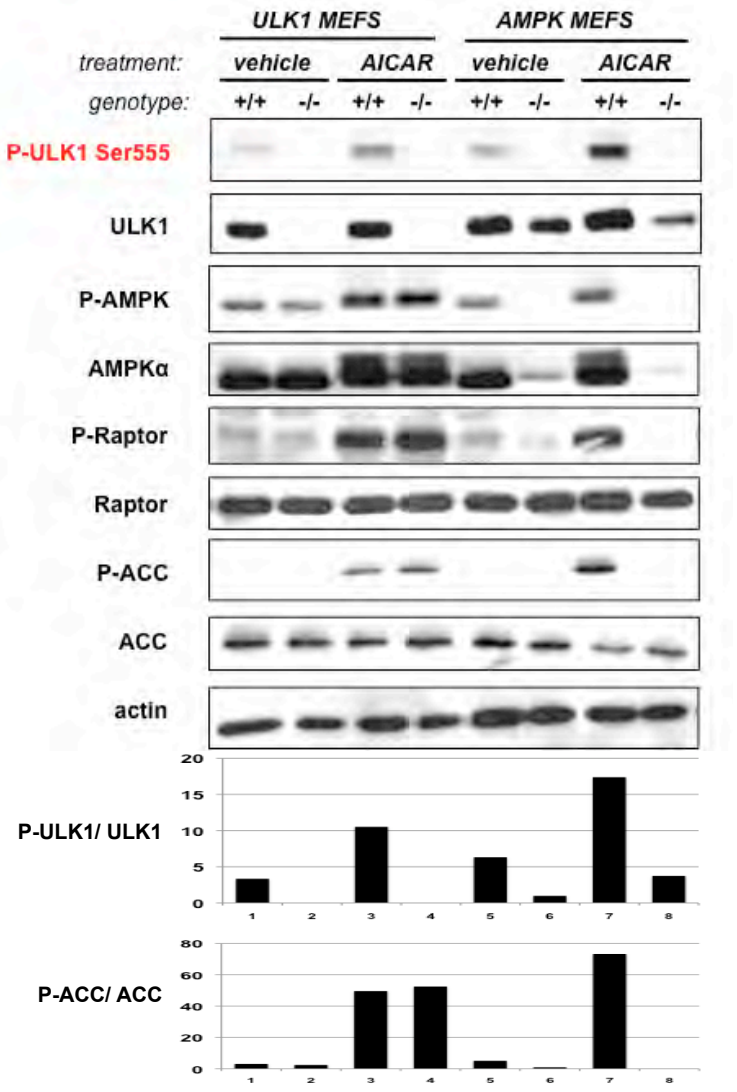

Fig. S6. Endogenous phospho ULK1 Ser_{555} increases with AICAR in primary MEFs. Endogenous ULK1 is phosphorylated on Ser_{555} in an AMPK- dependent manner following 2mM AICAR treatment for 1h in primary murine embryonic fibroblasts (MEFs). Phospho-ULK1, Phospho-ACC and total ULK1 and total ACC were quantified by densitometry and their ratios graphed. Data in all experiments is representative of 3 independent experiments.

Figure S7

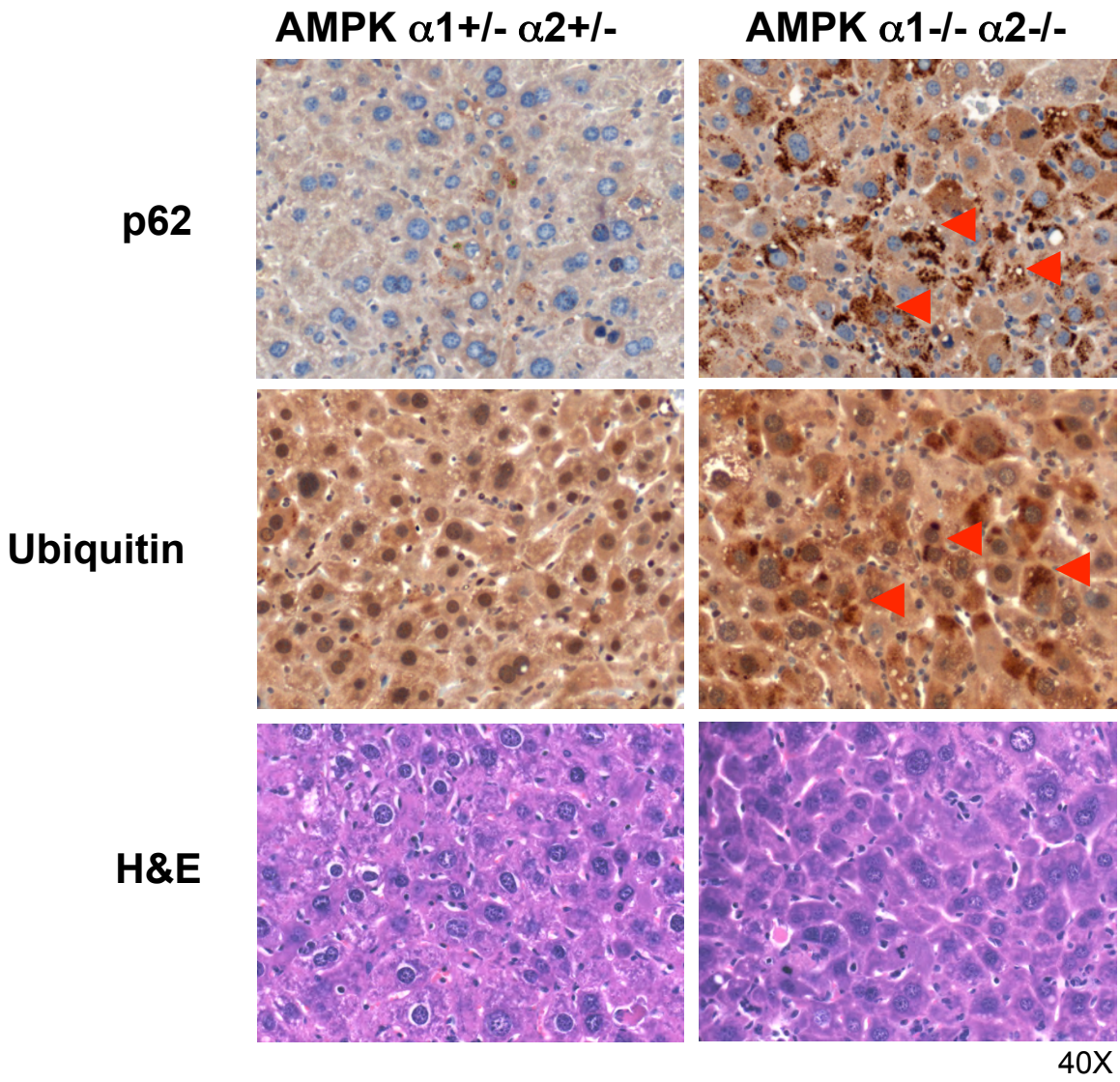

Fig. S7. p62 and ubiquitin are elevated in AMPK deficient livers compared to littermate controls as visualized by immunohistochemistry. AMPK deficient ($a1^{-/-}$; $a2^{lox/lox}$; tail-vein adenovirus cre-injected) livers or control ($a1^{+/-}$; $a2^{lox/+}$; tail vein adenovirus cre injected) livers were subjected to immunohistochemistry for the p62 autophagy marker or ubiquitin. Note elevated p62 and ubiquitin levels in the AMPK double knockout (DKO) liver. Overlapping aggregates of p62 and ubiquitin from serial sections indicated with red arrowheads. H&E is shown illustrating normal liver architecture. Data are representative of 2 independent experiments and 5 mice of each genotype analyzed.

Figure S8

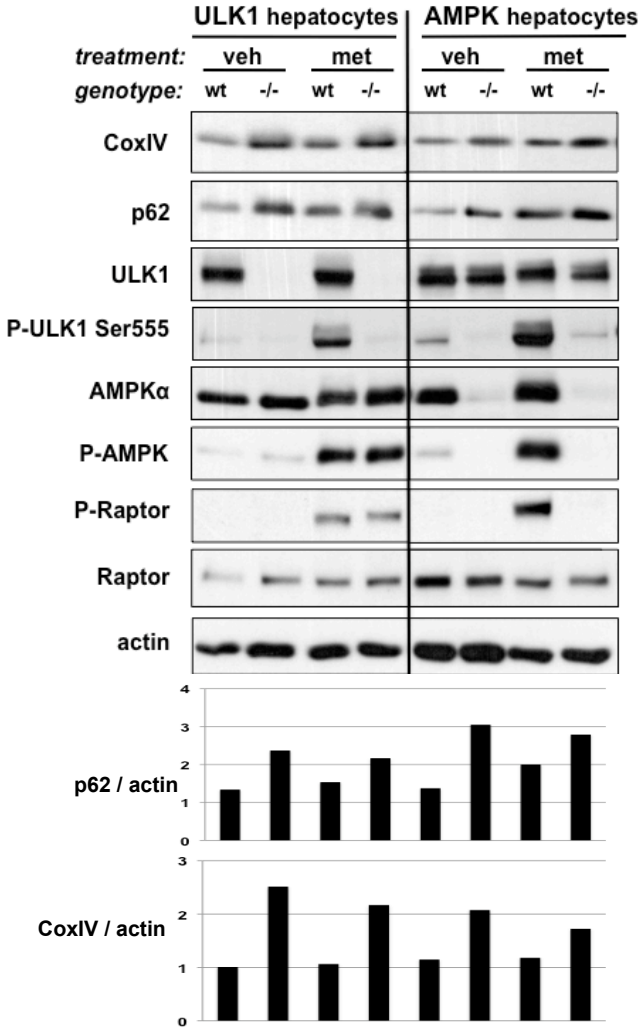

Fig. S8. p62 and the mitochondrial protein COXIV are elevated with loss of ULK1 or AMPK in primary murine hepatocytes.
Primary hepatocytes were derived from ULK1+/+ or ULK1-/- mice or aforementioned AMPK mice 7 days after tail-vein injection of adenovirus-cre. Cells were treated with 2mM metformin (met) or vehicle (veh) for 2h and immunoblotted with the indicated antibodies including p62 and the mitochondrial marker CoxIV, which are densitometrically quantified relative to actin below. Data is representative of 3 independent experiments.

Figure S9

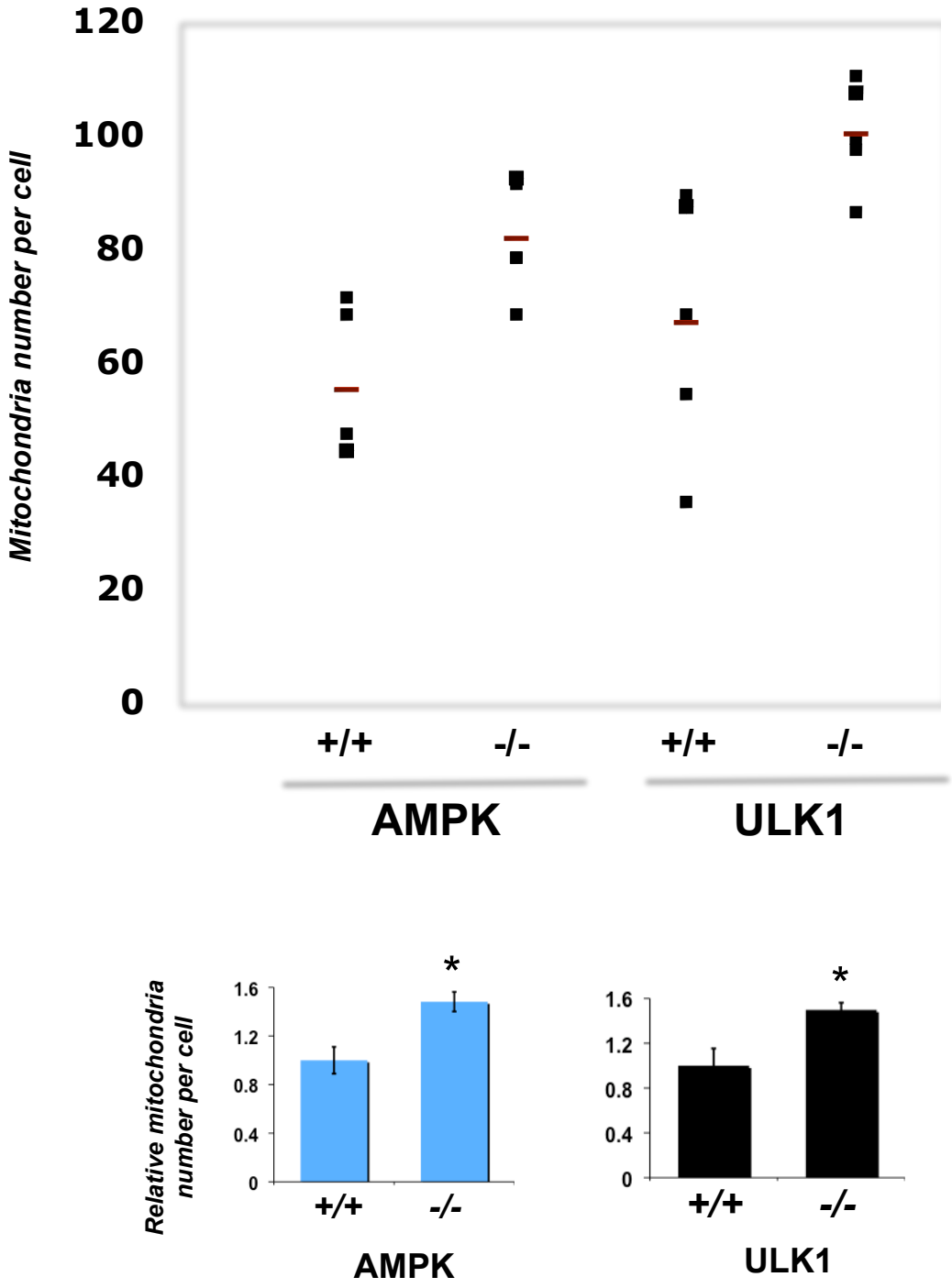

Fig. S9. Relative number of mitochondria are increased with loss of ULK1 or AMPK in primary murine hepatocytes. Quantification of TEM from primary murine hepatocytes from Fig. 2C. Top: boxwhisker plot of number of mitochondria per cell from 5 independent TEM fields. Below: The number of mitochondria per cell as expressed relative to levels seen in littermate matched control hepatocytes (set to 1.0). Data shown as mean +/- SEM. *P< .01 student's unpaired *t*-test

Figure S10

Data from Fig.Panel#	Strain	LGG-1::GFP expressing strain	RNAi treatment	Average # puncta/ seam cell	SEM	$N_{seam\ cells}$	$N_{animals}$	*P* value
3A1	MAH14	*daf-2(e1370)*	-	2.44	0.14	127	30	
			bec-1	0.67	0.08	155	17	<0.0001
			aak-2	0.82	0.12	135	16	<0.0001
			unc-51	1.08	0.11	181	25	<0.0001
3B2	DA2123	N2 wild-type	-	0.43	0.06	168	19	
			daf-2	1.41	0.14	112	16	<0.0001
	MAH28	*aak-2(ok524)*	-	0.57	0.06	237	29	
			daf-2	0.68	0.12	253	26	0.20
3C	DA2123	N2 wild-type	N/A	0.48	0.07	137	16	
	AGD383 'hets'	AAK-2::TOMATO	N/A	1.57	0.11	207	26	<0.0001
3D4	DA2123	N2 wild-type	-	1.07	0.14	74	8	
	AGD383 'hets'	AAK-2::TOMATO	-	3.37	0.15	223	34	
			unc-51	2.13	0.11	277	33	<0.0001

Fig. S10. Analysis of strains expressing the transgene LGG-1::GFP.
Summary of LGG-1::GFP positive puncta in L3 larvae of different genetic backgrounds using the LGG-1::GFP reporter (described in ref.15, and integrated in ref. 16). The average number of puncta per seam cell was calculated from two-three independent trials. $N_{seam\ cells}$, number of seam cells analyzed, $N_{animals}$, number of animals in which seam cells were analyzed. P values were calculated as unpaired, two-tailed t-test. N/A, animals were grown on regular OP50 E. coli bacteria. "hets' refer to F1 animals analyzed from cross between DA2123 and AGD383. Animals were raised at 20º. See Methods for more details.

Figure S11

Validating murine and human ULK2 shRNA lentis

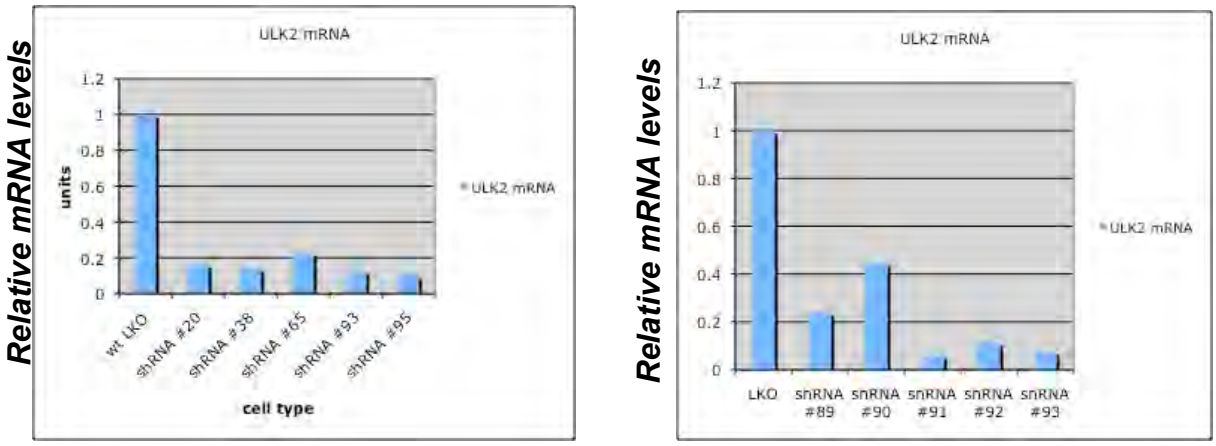

WT MEFs ***U2OS cells***

Validating human ULK1 shRNA lentis

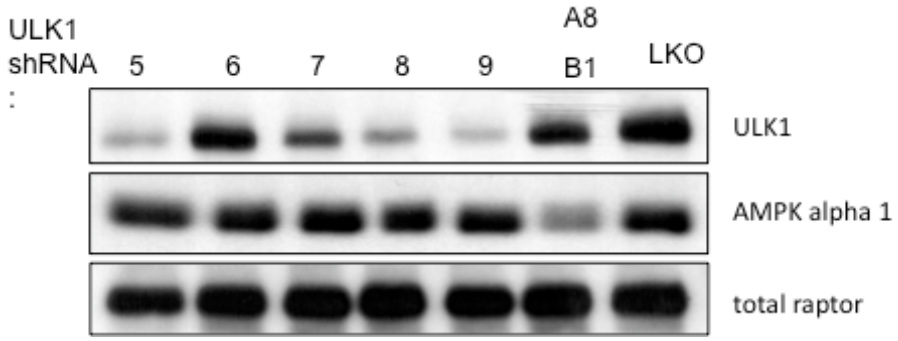

U2OS cells

Fig. S11. Validation of lentiviral shRNAs against human and murine ULK1 and ULK2. Top: Quantitative RT-PCR was used to validate the effectiveness of lentiviruses bearing hairpin shRNAs against murine and human ULK2 in cell types indicated. mRNA levels were normalized to GAPDH mRNA levels. Bottom: Immunoblotting was used to validate the effectiveness of lentiviruses bearing hairpin shRNAs against human ULK1. Lentivirus shRNAs A8/B10 directed against AMPKalpha served as a positive control for viral tittering and LKO is the empty lentiviral vector negative control. Raptor served as a loading control here.

Figure S12

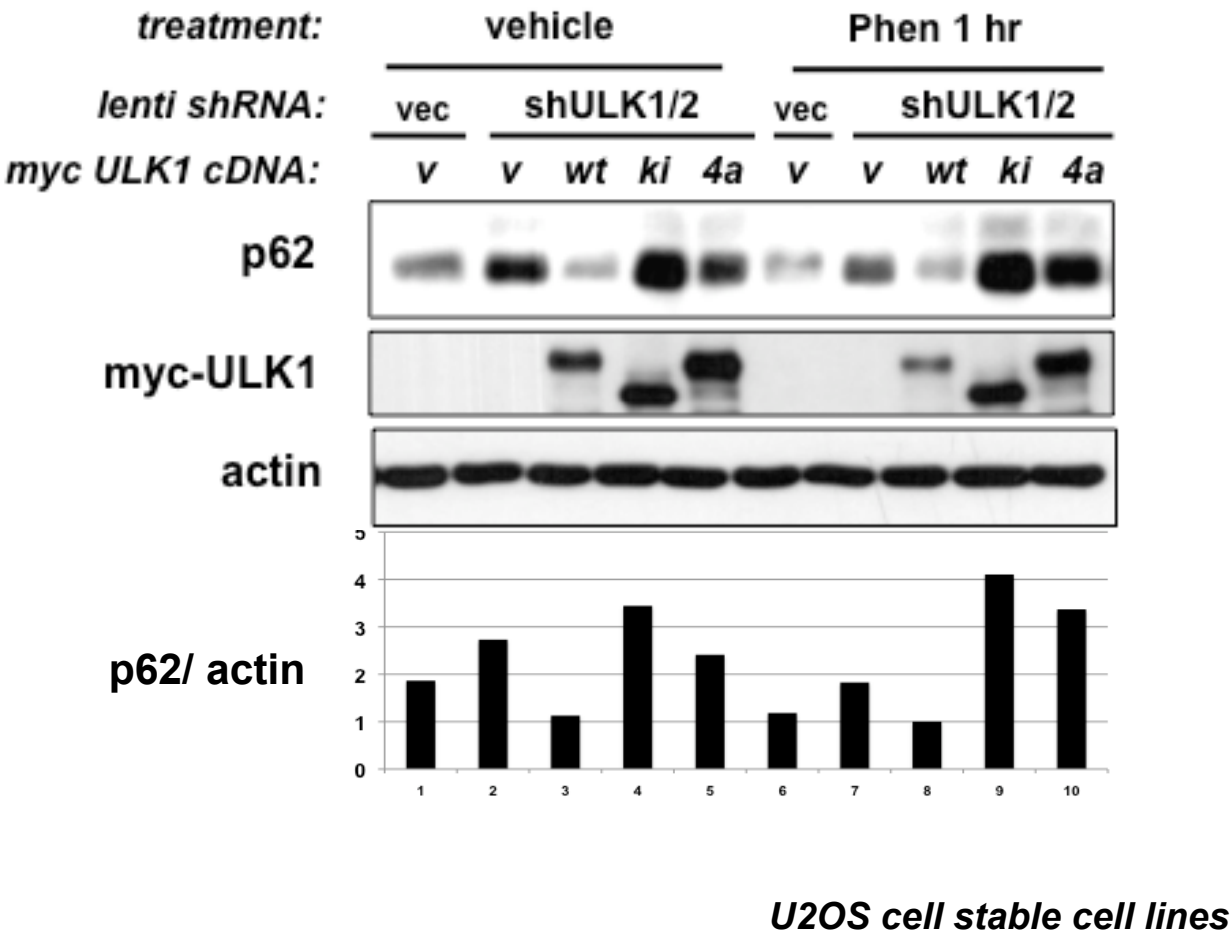

Fig. S12. U2OS cells lacking ULK1/2 function is mirrored by mutation of the AMPK sites in ULK1 and these sites are required for ULK1 function.
U2OS cells were stably infected with empty lentiviral vector pLKO (vec) or human ULK1 and ULK2 shRNA-expressing lentiviruses and then stably reconstituted with retroviruses bearing wild-type (WT) or kinase-inactive (KI) or AMPK non- phosphosphorylatable (4SA) ULK1 cDNA or the empty retroviral vector (v). WT ULK1, but not KI or 4SA ULK1 was able to restore p62 degradation to the ULK1/2-deficient U2OS cells, which is quantified by densitometry below (detailed in methods). Cells were treated with 5mM Phenformin (Phen) or vehicle for 1h. Results are representative of 3 independent experiments.

Figure S13

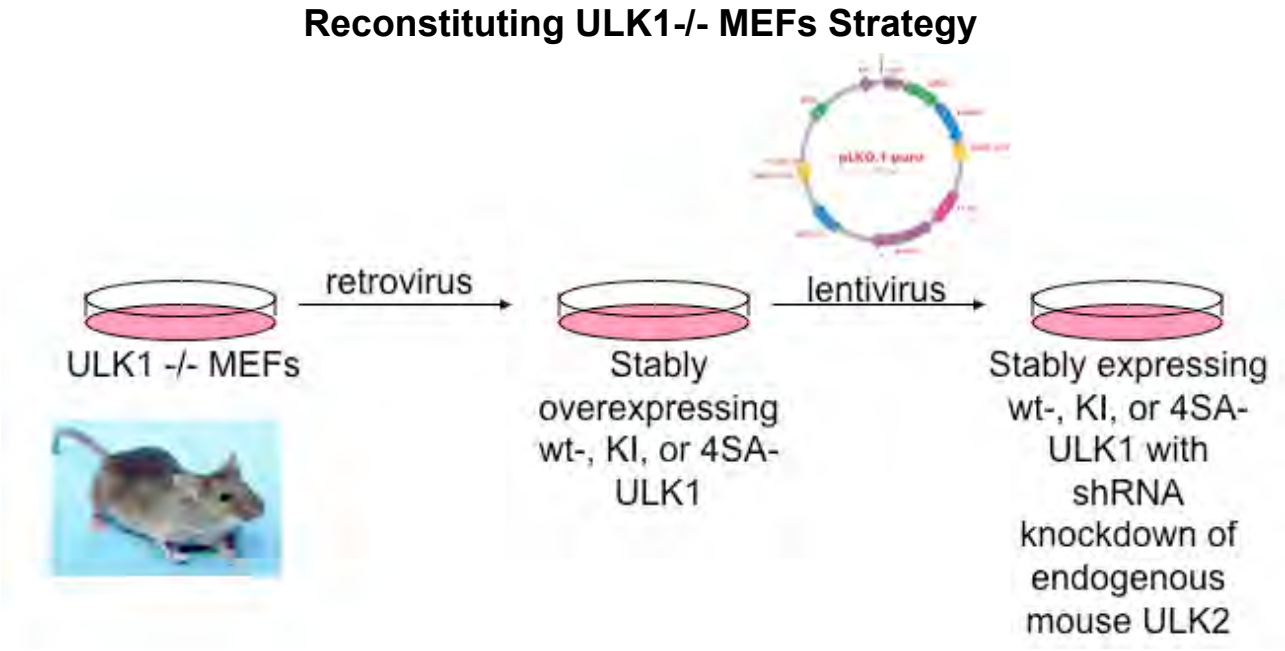

Fig. S13. Reconstitution strategy for ULK1-/- MEFs.
Retroviruses bearing myc-tagged wild-type or kinase inactive or non-phosphorylatable ULK1 were introduced into ULK1-/- MEFs and after selection these cells were next infected with lentiviruses bearing shRNAs for murine ULK2. The same strategy was used for replacing ULK1/2 function in U2OS cells except there after the retroviral selection, cells were co-infected with lentiviruses bearing shRNAs against human ULK1 and ULK2.

Figure S14

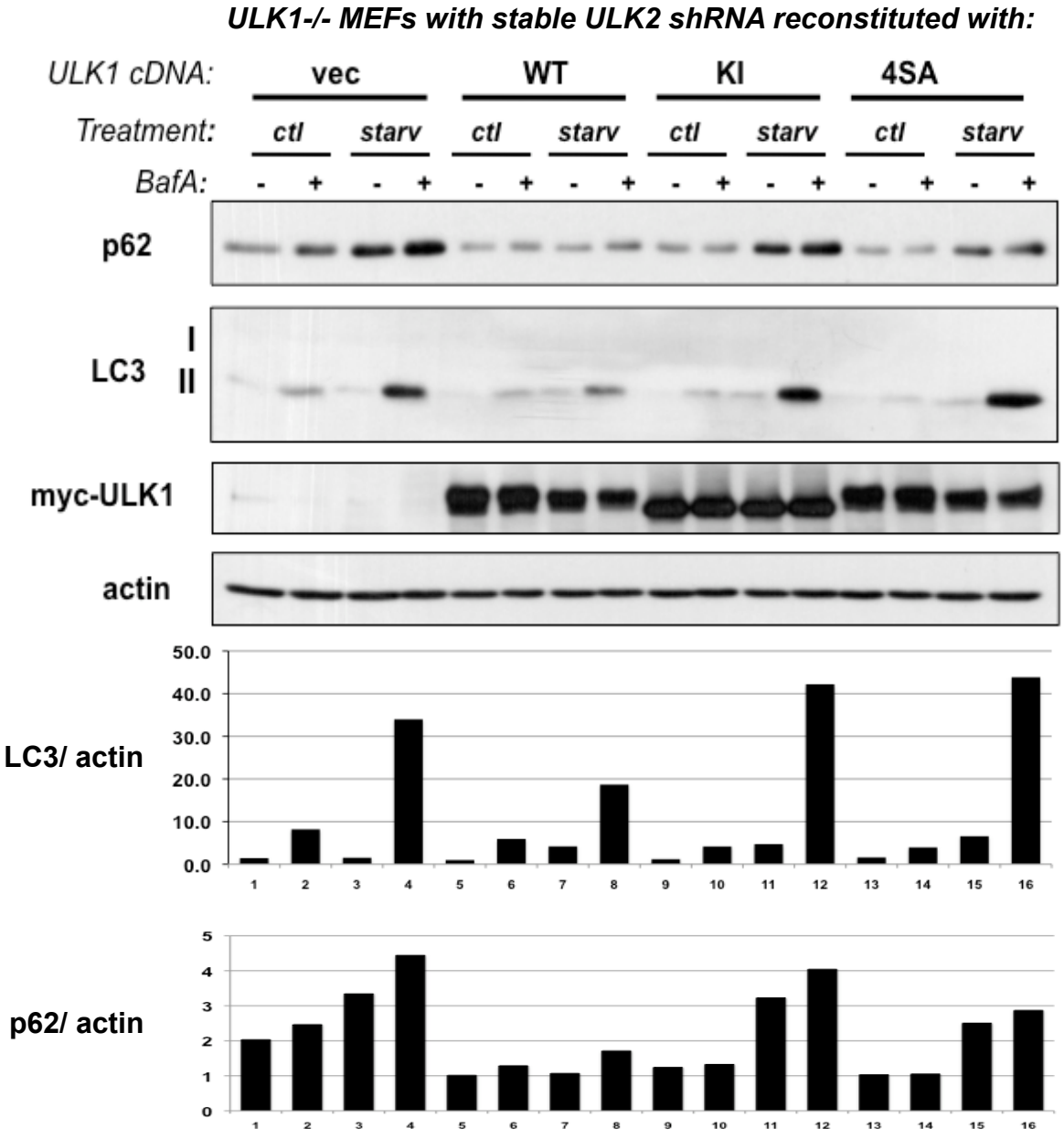

Fig. S14. MEFs lacking ULK1/2 function is mirrored by mutation of the AMPK sites in ULK1 and these sites are required for ULK1 function.

ULK1-/- MEFs bearing stable murine ULK2 shRNA lentiviruses were stably reconstituted with retroviral vectors bearing WT, KI, or 4SA ULK1 or no cDNA (vec) and then placed in starvation media (starv – EBSS: Earle's buffered salt solution) or control media (ctl: standard media for these cells: DMEM + 10% FBS) for 6h in the presence of BafilomycinA (BafA) as indicated. Lipidated LC3 (II) and p62 levels were quantified by densitometry and shown at bottom. Results are representative of 3 independent experiments.

Figure S15

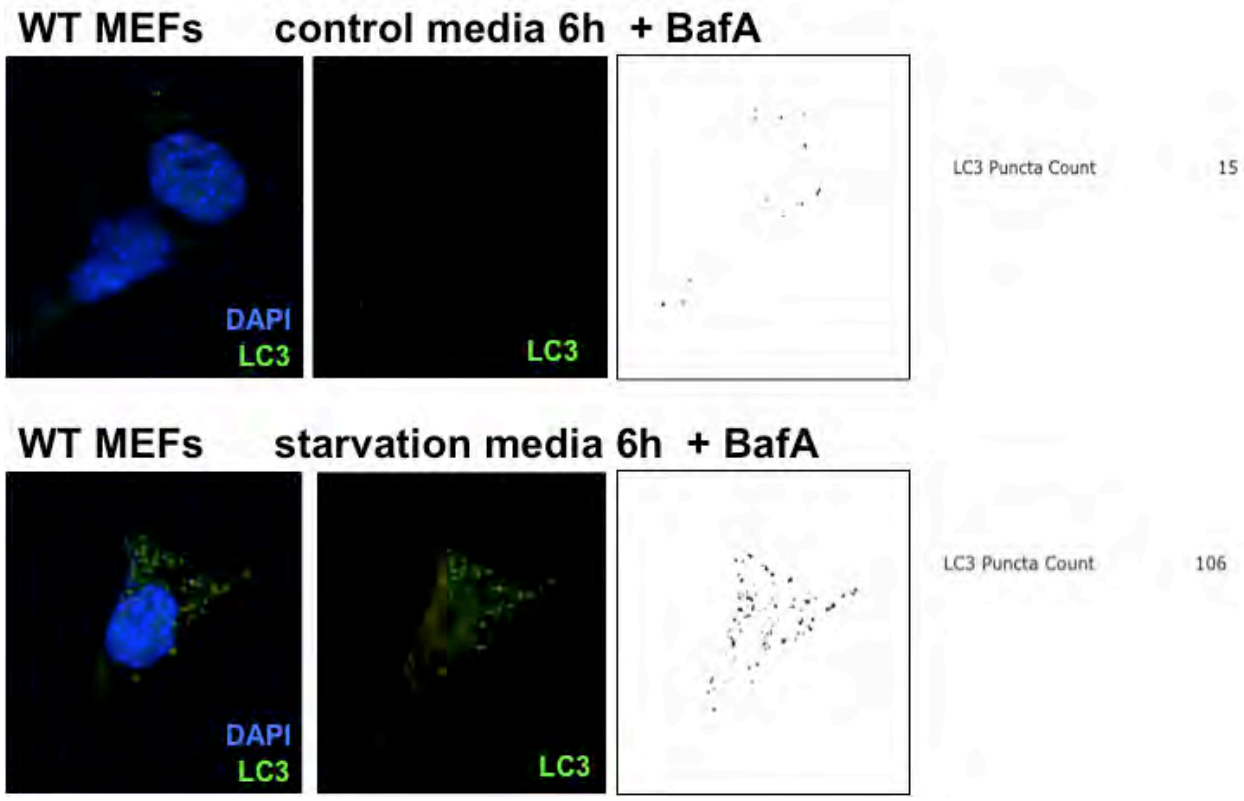

Fig. S15. Measuring LC3 punctae using ImageJ macro morphometric software. Starvation in EBSS media in our MEF cell model induces endogenous LC3 punctae which can be measured and quantified using anti LC3 antibody (Cell Signaling #3868) and subsequent ImageJ quantification of immunocytochemistry. Data representative of cells from > ten 63X fields.

Figure S16

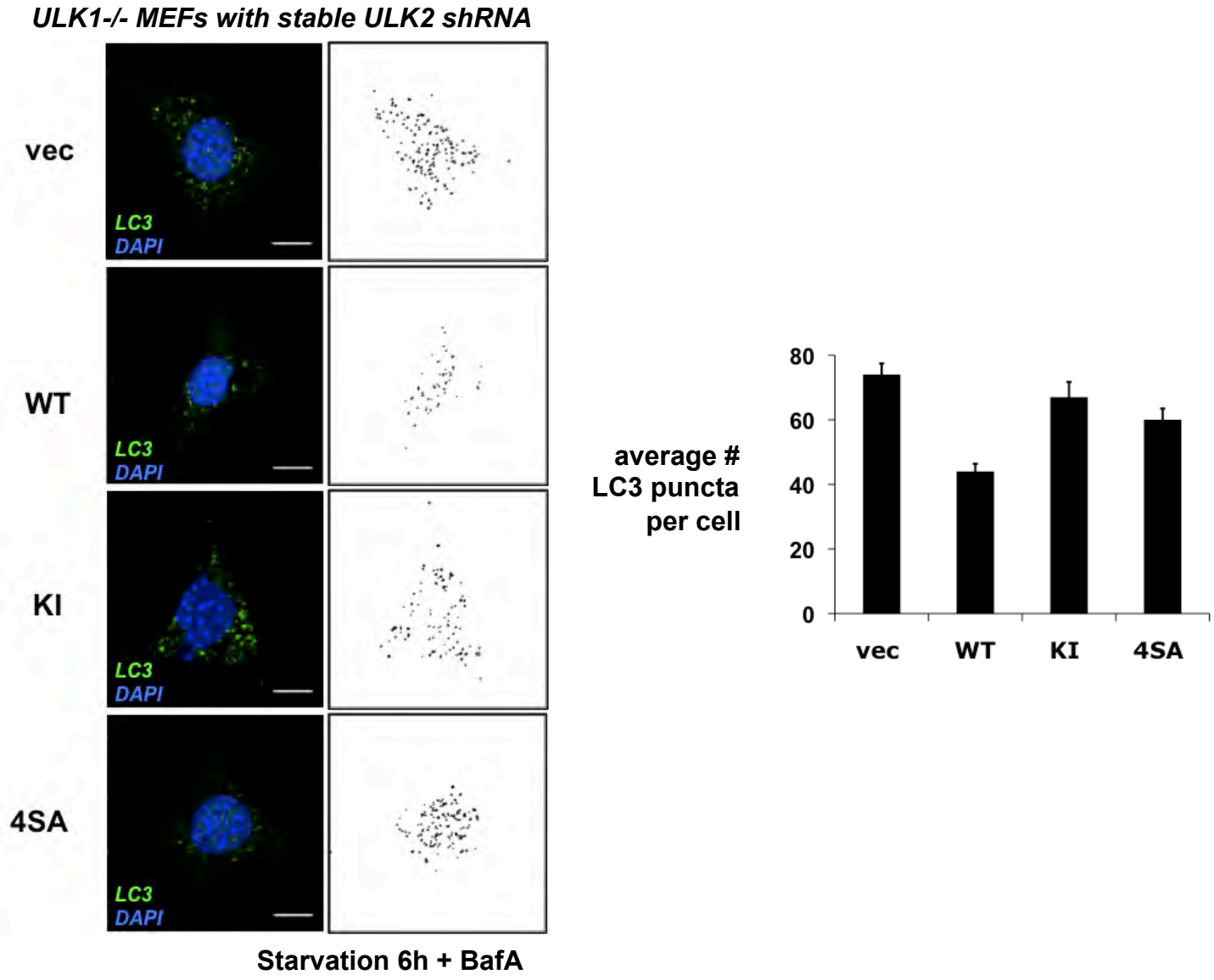

Fig. S16. MEFs lacking ULK1/2 function is mirrored by mutation of the AMPK sites in ULK1 with regard to endogenous LC3 staining after starvation.
Localization of endogenous LC3 in 6h starved (EBSS) BafA treated cells from Fig 4B. LC3 was localized to puncta following placement of MEF cells into starvation medium. LC3 positive puncta were quantified using an LC3 ImageJ macro as outlined in Fig. S15. Ten 63xfields per condition were quantified. In contrast to p62, ULK1-defiency did not prevent endogenous LC3 lipidation or puncta formation in this cell type, consistent with previous findings that neither ULK1- nor AMPK-deficiency impact LC3 conversion in MEFs (refs. 5, 8, and 22).

Figure S17

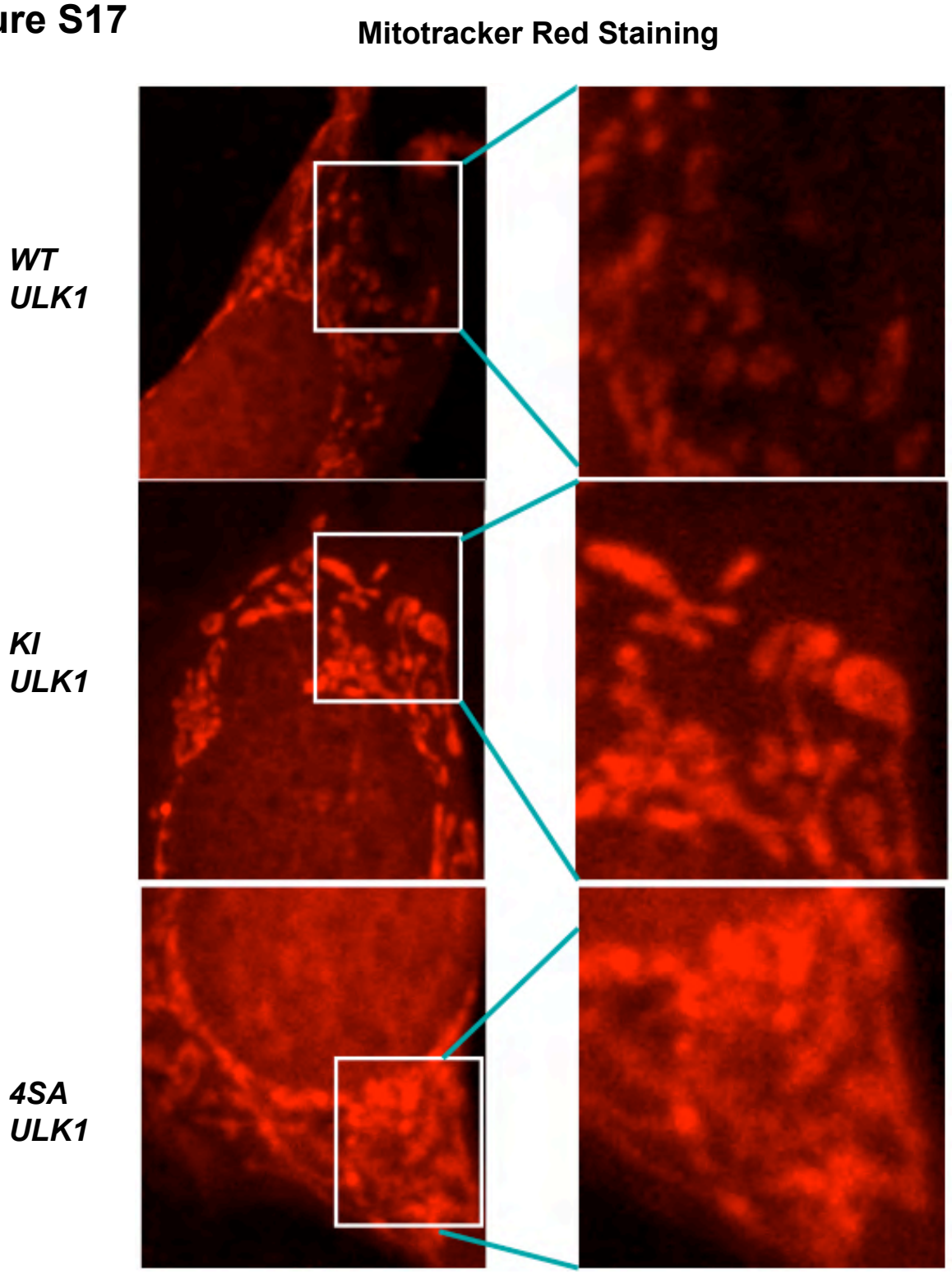

Fig. S17. Mitotracker staining of ULK1 cDNA-reconstituted ULK1-/- MEFs
Mitotracker Red CMXRos staining of mitochondria used at 50 nM for 15 min. Images from WT, KI, or 4SA reconstituted ULK1- /- MEFs bearing ULK2 shRNA taken on confocal microscope as described in methods.

Figure S18

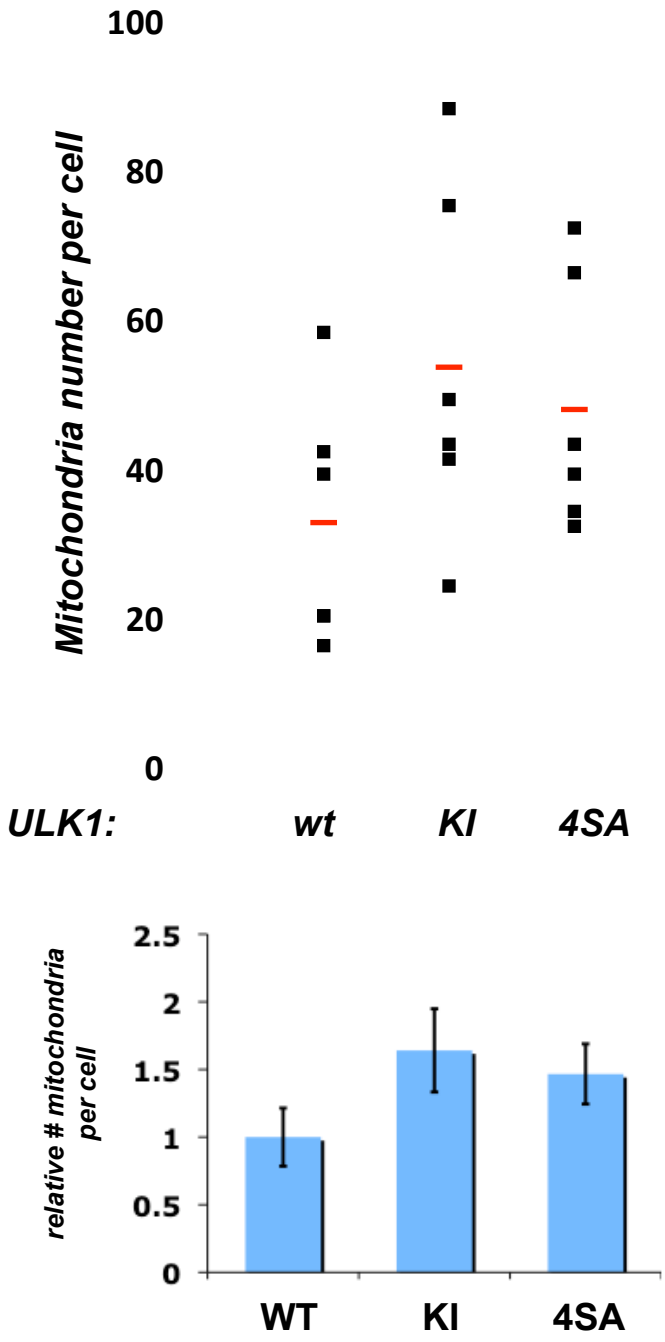

Fig. S18. Relative number of mitochondria are increased with loss of ULK1/2 function. Quantification of the number of mitochondria per cell from Fig. 4C as analyzed using Inform morphometric software as in Fig. S8. Details in methods. Cells expressing WT ULK1 were set to 1.0 (=avg 32.5 mito/cell).

Figure S19

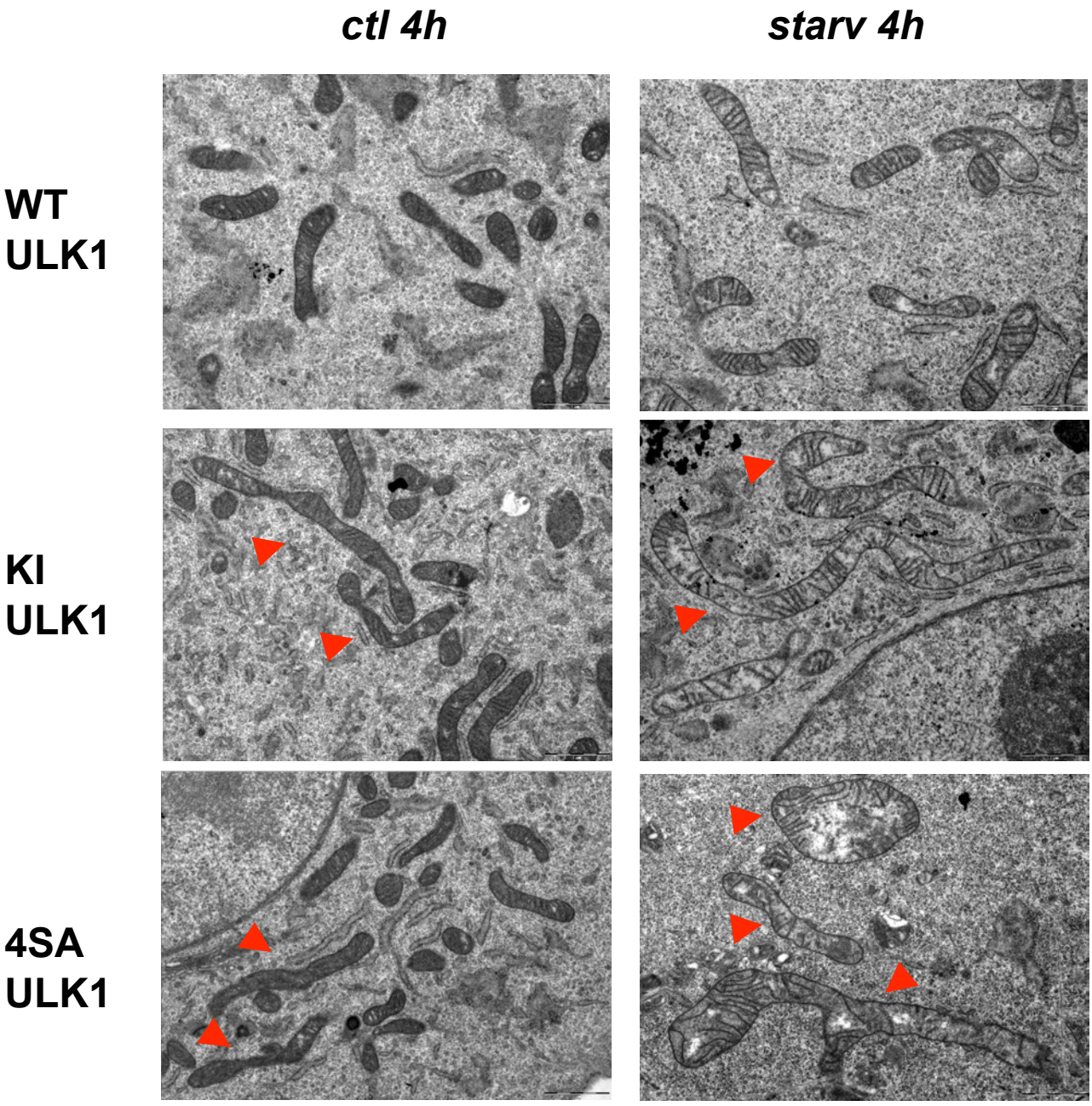

Fig. S19. Mitochondrial defects in ULK-deficient MEFs reconsitutued with KI or 4SA mutant ULK1. Transmitting Electron Microscopy images from WT, KI, or 4SA reconstituted ULK1-/- MEFs bearing ULK2 shRNA. Cells were placed into fresh growth media (ctl) or EBSS (starvation) at time zero and fixed at 4h. Note the aberrant elongated mitochondria in the KI and 4SA cells, and the altered mitochondrial cristae in the KI or 4SA reconstituted cells following starvation. Images taken at 13,500x.

Figure S20

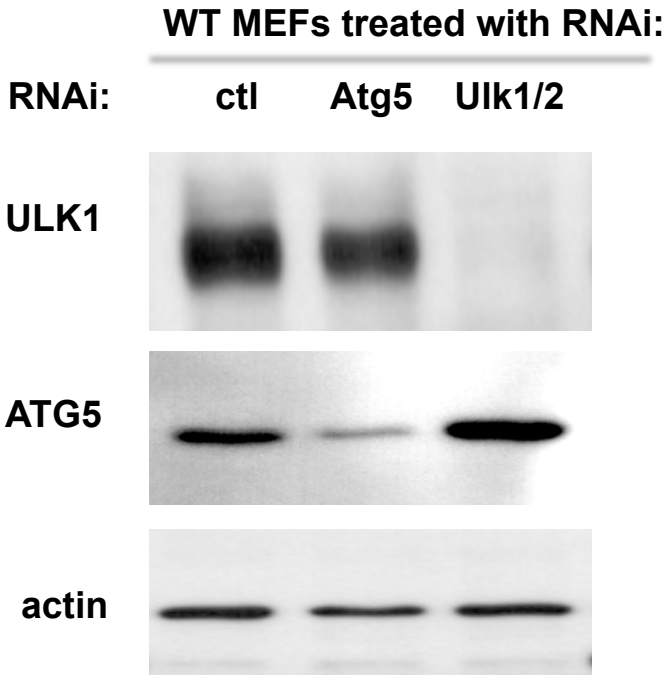

Fig. S20. Validation of Dharmacon smartpool siRNAs against murine ULK1, ULK2, and Atg5.
Wild-type (WT) MEFs transfected with 20nM siRNA pools to a universal control (ctl), murine Atg5, or murine ULK1 and ULK2 for 72 hours. Proteins from lysates were immunoblotted with indicated total antibody.

Figure S21

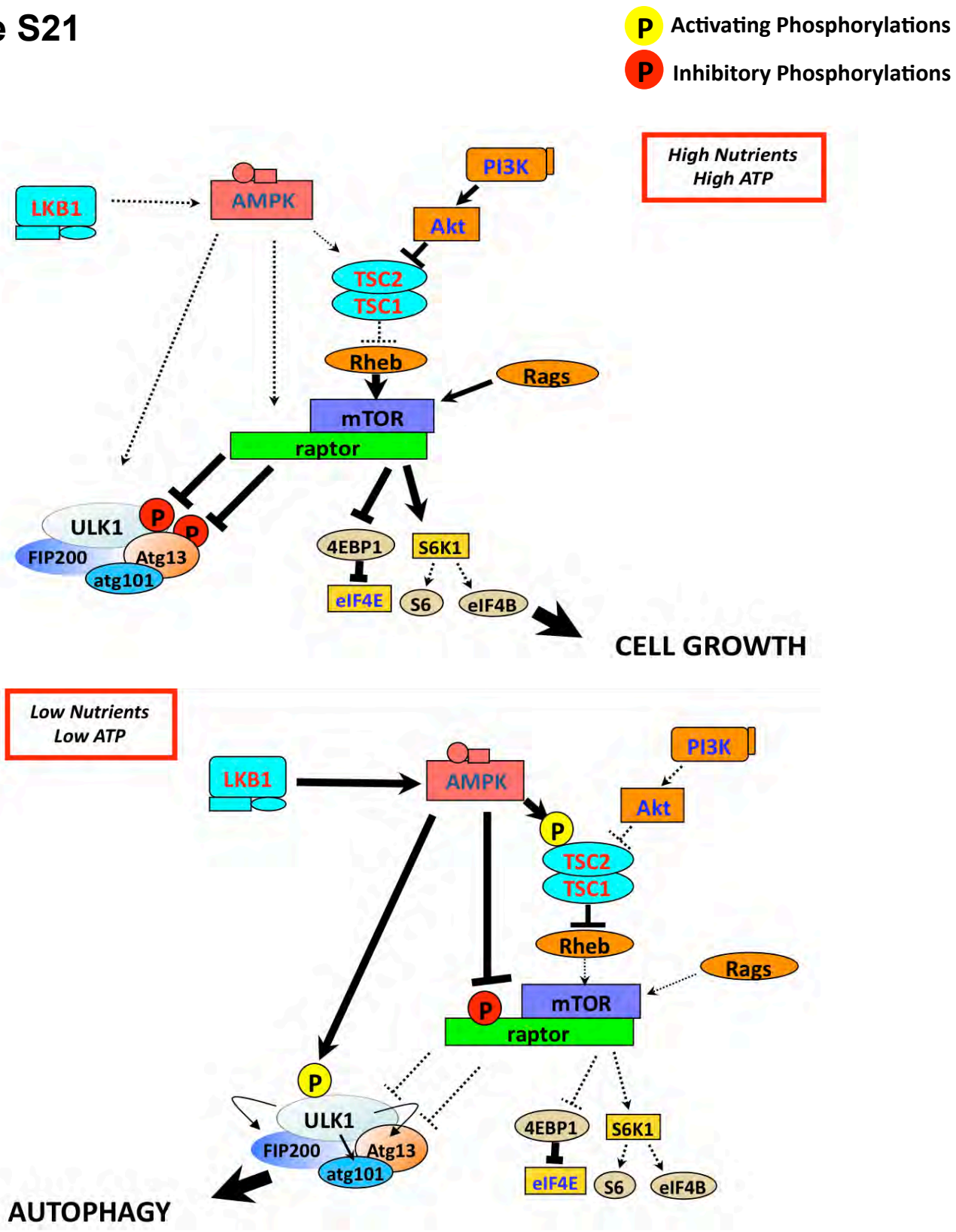

Fig. S21. Model for AMPK and mTOR regulation of the activity of the ULK1 complex via opposing phosphorylation events. Schematic of intersection of mTOR, AMPK, and ULK1 pathways. Top: Under nutrient replete conditions. Bottom: Under nutrient deprived conditions.